

## Towards reliable charge-mobility benchmark measurements for organic semiconductors



James C. Blakesley<sup>a,\*</sup>, Fernando A. Castro<sup>a</sup>, William Kylberg<sup>a</sup>, George F.A. Dibb<sup>a</sup>,  
Caroline Arantes<sup>b</sup>, Rogério Valaski<sup>b</sup>, Marco Cremona<sup>b,c</sup>, Jong Soo Kim<sup>d</sup>, Ji-Seon Kim<sup>d</sup>

<sup>a</sup> National Physical Laboratory, Teddington TW11 0LW, United Kingdom

<sup>b</sup> Divisão de Metrologia de Materiais, INMETRO, Xerém, Duque de Caxias, RJ 25250-020, Brazil

<sup>c</sup> Physics Department, Pontifícia Universidade Católica do Rio de Janeiro, Rio de Janeiro, RJ 22453-970, Brazil

<sup>d</sup> Department of Physics, Imperial College, London SW7 2AZ, United Kingdom

### ARTICLE INFO

#### Article history:

Received 22 October 2013

Received in revised form 10 February 2014

Accepted 11 February 2014

Available online 26 February 2014

#### Keywords:

Mobility

Space-charge limited current

Injection-limited current

Charge-carrier mobility

Mobility benchmark

### ABSTRACT

Charge carrier mobility is a figure of merit commonly used to rate organic semiconducting materials for their suitability in applications such as solid-state lighting or photovoltaics. Although large variations are found in published mobility values on identical materials, there is little open discussion in the literature of the reproducibility of these results. We address this with an interlaboratory study of mobility measurements performed on a set of organic semiconductors using the space-charge limited current method. We found mobility measured on nominally identical devices could vary by more than one order of magnitude, with the largest sources of variation being poor electrodes and film thickness variation. Moreover, we found that mobility values extracted from identical data by different scientists would typically vary by a factor of 3. We propose a protocol for analysis and reporting that was found to reduce this analysis variation to as little as 20%. We also present general guidelines for improving the reproducibility of benchmark mobility measurements.

Crown Copyright © 2014 Published by Elsevier B.V. This is an open access article under the CC BY-NC-SA license (<http://creativecommons.org/licenses/by-nc-sa/3.0/>).

### 1. Introduction

Organic semiconductors are used in the emerging organic electronics industry as the essential active materials for functional devices such as organic thin-film transistors (OTFTs), organic photovoltaics (OPVs) and organic light-emitting diodes (OLEDs). As the industry evolves, there is an increasing demand for simple, reproducible measurements of the critical material parameters that affect device performance. These are typically used to optimise processes or to assess the potential of new materials in research and development programmes, or as quality control for material production.

Charge transport in organic semiconductors is critical to good device performance. In OPVs, efficient, balanced charge transport reduces current losses from recombination and series resistance losses under high irradiances [1–4]. In OLEDs, good charge transport is important for achieving a combination of high efficiency and high brightness [5]. Charge transport in organic semiconductors has been described by models of varying complexity, including device-level and molecular-level models requiring many parameters [6–10]. However, engineers focussed on applications often favour reduction to a simpler description with a single parameter that can be used to benchmark and compare different materials. Typically the preferred parameter is ‘mobility’ – the mean charge velocity divided by the electric field.

In disordered materials, such as typical organic semiconductors or amorphous inorganic materials, care needs

\* Corresponding author.

E-mail addresses: [james.blakesley@physics.org](mailto:james.blakesley@physics.org), [james.blakesley@npl.co.uk](mailto:james.blakesley@npl.co.uk) (J.C. Blakesley).

to be taken with the concept of mobility. Scher and Montroull noted in 1975 that “...the simple notion of a mobility, field dependent or otherwise, is very limited.” [11] Orders of magnitude variations in mobility values measured on the same material using different techniques are common and widely accepted in the field; though they are not often candidly discussed, and even less often quantified. Nevertheless, mobility measurements can be useful for screening applications if properly used. In the context of a small interlaboratory study of mobility measurements on a set of organic semiconductors, this paper is intended to help readers to understand and manage some of the uncertainties in mobility measurements. The focus is on mobility measurements applicable to diode structures, such as OLED and OPV devices. The results do not apply to OFETs, which operate in a completely different transport regime [12,13] and have relatively harmonised measurement procedures. We briefly discuss the challenges and advantages of different techniques and focus on the simplest and most versatile method: the space-charge limited current–voltage (SCLC) technique. We identify the major sources of experimental errors that affect device reproducibility. Strikingly, we demonstrate that different approaches to data analysis are one of the major sources of uncertainty when extracting mobility data from these measurements. To tackle this issue and improve reproducibility of measurements, we propose a protocol for data analysis and show that standard deviation can be significantly reduced.

In Section 2 of this paper we describe the fabrication of devices used for experimental studies. In Section 3 we briefly compare different methods of measuring mobility in diode structures. In Section 4 we report on the reproducibility of the SCLC technique and propose a protocol for data analysis. In Section 5 we use sensitivity analysis to analyse the sources of variation in SCLC mobility measurements. In section 6 we discuss and summarise our conclusions. Readers who are familiar with the SCLC technique may wish to skip directly to Section 4, 5, or 6.

## 2. Device fabrication

Sandwich-type devices were fabricated by spin-coating organic semiconductor films of different thicknesses (from 60 nm to 1100 nm) from toluene solution onto patterned transparent indium tin oxide (ITO) coated glass substrates coated with poly(3,4-ethylenedioxythiophene) doped with poly(styrenesulfonate) (PEDOT:PSS) (Clevios AI4083). These were capped with thermally evaporated top electrodes, defining active device areas of 0.04 cm<sup>2</sup> overlap between the top electrode and ITO.

For the semiconductor layer, three fluorene-based alternating copolymers were studied: F8BT, TFB and PFB (see supplemental information for chemical structures [14]). Previous studies of similar materials have found hole transport to be relatively poor, and characterised by strong energetic disorder [6,15,16]. They present an interesting challenge for studying charge transport measurements, as mobility is predicted to vary with electric field, charge density and time (under transient conditions), and were chosen to present a “worst-case” scenario. These materials

are anecdotally reported to be relatively air stable. The approximate highest occupied molecular orbital (HOMO) and lowest unoccupied molecular orbital (LUMO) energies are displayed in Fig. 1. PEDOT:PSS acts as a transparent hole-injection layer (HIL) and electron-blocking layer with a work function of around 5.1–5.3 eV [17]. For some materials, an energetic barrier is expected for hole injection from PEDOT:PSS (i.e. 0.5–0.9 eV barrier for F8BT). Gold was used as a top electrode. The Fermi level of gold (work function  $\sim$ 4.5 eV under these conditions [18,19]) is expected to lie within the band gap of all three materials, presenting an energetic barrier to injection of both electrons and holes. A duplicate set of devices was created with a 5 nm interlayer of MoO<sub>3</sub> thermally deposited between the polymer semiconductor layer and the gold top electrode. MoO<sub>3</sub> acts as a HIL with a high work function (between 5.6 eV and 6.8 eV [20]) that is sufficient to inject holes efficiently into most conjugated polymers, including F8BT [16,21].

Devices were fabricated in nitrogen-filled glove boxes. For interlaboratory studies, duplicate sets of devices were fabricated at the same time and transported in vacuum-sealed packages. Devices were stored in nitrogen- or argon-filled gloveboxes and measured in air-tight containers filled with gas from the gloveboxes. During transport and measurement of the devices, monitoring of the quality of the atmosphere was impossible. These conditions are typical of those used for research and development in the field.

## 3. Mobility measurement techniques

In our initial study, mobility measurements were performed at different laboratories using a range of techniques. These were the steady-state space-charge limited current (SCLC) method and the transient methods: time-of-flight (ToF), dark-injection transient current (DITC) and charge extraction by linearly increasing voltage (CELIV). SCLC was the only technique that was able to extract a mobility measurement on every device. However, as we describe below, this does not necessarily mean that the extracted mobility values were consistent. The transient

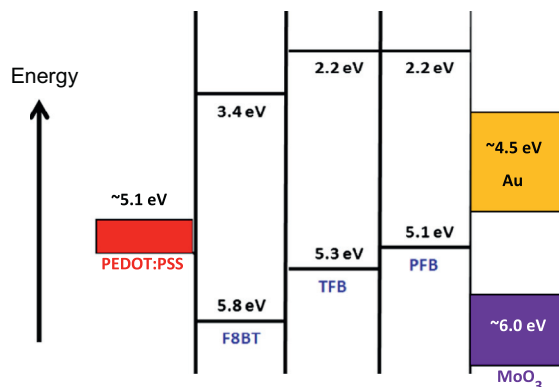


**Fig. 1.** Approximate energy-level alignment diagram showing the LUMO and HOMO energies of the three organic semiconductors studied and the Fermi levels of three electrode materials. Note that typical uncertainties on these values are  $\pm 0.2$  eV.

techniques were found to be less versatile, and only gave results when specific conditions were met.

The mobility values measured by transient techniques (not shown) were higher than the highest SCLC measurements by as much as a factor of 10. This can be explained by charge trapping, or other forms of anomalous dispersion, in which charge carriers undergo relaxation on the timescale of the experiment [22–25]. Such relaxation can occur progressively over a broad range of timescales, leading to a continual decrease of mobility with time over several orders of magnitude [26–28] and the measured mobility can depend on the conditions of the experiment, such as electric field and film thickness [29]. While some reports have successfully combined different transient techniques using multiparameter models to extract detailed information about trap states in materials [6,28,30,31], these approaches are typically too specialised for use in general material screening applications. We briefly describe the reasons for the lack of versatility of the transient techniques: ToF measurements require that photogenerated charge is produced close to one electrode, and that the transit time of carriers is greater than the RC constant of the measurement circuit. This prevents measurement of films thinner than  $\sim 1 \mu\text{m}$ . Films must also be sufficiently non-conductive [32]. DITC measurements [33] suffer from problems with capacitive effects that create difficulties for measurements on thin films. On thicker films, transient features may be too weak to measure, or can disappear altogether due to charge trapping [34]. CE-LIV requires films to be sufficiently conductive [32]. In the study reported here, the intrinsic carrier density plus photocarriers generated by background light were insufficient to produce a measurable signal. Bias light or pulsed excitation can be used, although this introduces additional complexity. Also, the polarity of the measured charge carriers cannot be identified.

We therefore argue that the SCLC technique is most versatile for material benchmarking applications, with the possible exception of some high electron-mobility materials in which electron injection can be problematic [35–37]. It also has the advantages of modest equipment requirements and, being steady state, reproducing conditions relevant to the application in OLED and OPV devices. For this reason, we performed a study to investigate the limitations of using this technique specifically for the purpose of making comparisons between materials, formulations, or processes. Here, accuracy is less important than reproducibility. Accuracy is also difficult to quantify; the reduction of charge transport to a single mobility value is an oversimplification. Thus, we refer to the single value extracted from SCLC measurements as a ‘mobility benchmark’.

For SCLC measurements, a hole-only or electron-only diode device structure is required. At least one electrode must efficiently inject the required charge carrier, while the other must block injection of charge carriers of the opposite polarity. When a voltage is applied to the diode, unipolar charge is injected into the semiconductor film, resulting in a build-up of space-charge [38]. Given sufficient time (greater than the carrier transit time), the space-charge is sufficient to diminish the electric field at

the injecting contact, and the amount of charge inside the device saturates. New charge is injected only to replace charge that is extracted at the opposite electrode. Assuming a uniform charge-carrier mobility, the steady-state current density  $J_{\text{SCLC}}$  is theoretically a function of the applied voltage  $V$ , the film thickness  $d$ , the permittivity of the film  $\epsilon$ , and the steady-state charge-carrier mobility  $\mu_{\text{SCLC}}$ :

$$J_{\text{SCLC}} = \frac{9}{8} \mu_{\text{SCLC}} \epsilon \frac{V^2}{d^3}, \quad (1)$$

In reality, the mobility commonly varies with electric field. For this reason, a modification to this model developed by Murgatroyd [39] is used, in which the mobility is assumed to take the form:

$$\mu = \mu_0 \cdot \exp(\gamma \sqrt{F}), \quad (2)$$

where  $\mu_0$  is a new parameter representing the mobility in the limit of zero electric field,  $\gamma$  is a parameter that describes the strength of the field-dependence effect, and  $F$  is the electric field. This general field dependence of mobility can arise from shallow trapping or disorder [22]. It can also hide other effects, such as carrier-density dependent mobilities and deep trapping, which can only be separated by more detailed modelling combined with experiments covering a large parameter space [6,15,16,40,41]. Taking into account that the electric field is not constant throughout the film, Murgatroyd approximated the SCLC current density to:

$$J_{\text{SCLC}} = \frac{9}{8} \epsilon \frac{V^2}{d^3} \mu_0 \cdot \exp\left(0.89 \gamma \sqrt{\frac{V}{d}}\right). \quad (3)$$

SCLC mobility measurements are typically performed by measuring steady-state current–voltage ( $I$ – $V$ ) curves and fitting with either of Eqs. (1), or (3) by varying the fit parameters ( $\mu_{\text{SCLC}}$  or  $\mu_0$  and  $\gamma$ ) with other parameters ( $V$ ,  $d$ , AND  $\epsilon$ ) known or assumed. The advantage of Eq. (3) is that it is able to fit a broader range of  $I$ – $V$  curves. The disadvantage is that an additional parameter is required, adding uncertainty and confusing comparisons between materials.

The most important assumptions of the theory are as follows:

- *Charge injection is efficient:* the injecting electrode must be capable of injecting sufficient current into the organic semiconductor film to maintain a current that is bulk-limited rather than interface-limited. This is generally achieved by using an electrode that has a work function aligned to the desired HOMO or LUMO level of the semiconductor and has a low contact resistance. As injection limited behaviour can have similar characteristics to space charge limited behaviour, this condition can be difficult to verify experimentally and can lead to false mobility measurements. Poor charge injection becomes a more serious issue in thinner films, where more current is required to sustain SCLC. For any electrode/semiconductor combination there will be a minimum thickness at which SCLC measurements can be successfully made. For many measurements, there will also be a minimum voltage required to achieve SCLC [42].

- *Series resistance does not dominate:* Similar to the above, external series resistances (e.g. from thin-film electrode materials used for contacting) can reduce the voltage dropped across the semiconductor film when the current is high. This is often identified by the current–voltage curve becoming linear at high voltages. This is particularly an issue where thin films of high mobility materials are to be characterised. There are several strategies for dealing with this problem, including: using four-wire current–voltage measurements, using thicker films to reduce the overall current, and designing device geometry to maximise the ratio of conductor width to active area.
- *Devices are unipolar:* For hole-only devices, the injection of electrons from the collecting electrode must be blocked and *vice versa* for electron-only devices. This can be verified by comparing different electrodes combinations (see below). Checking for light emission is a common test for bipolar charge transport; emission of visible light under an applied voltage indicates that electron–hole recombination is occurring inside the device, and therefore is unsuitable for SCLC mobility measurements. However, the absence of visible emission does not necessarily guarantee unipolar behaviour.
- *Built-in voltage and  $\epsilon$  are known:* Diode structures usually contain built-in voltage  $V_{BI}$  due to mismatch between the two electrode work functions and interfaces, even when the electrode materials are nominally the same.  $V_{BI}$  is difficult to measure, but can be estimated. If  $V_{BI}$  is known, it can be compensated for by applying an offset to the voltage  $V = V_{ext} - V_{BI}$ , where  $V_{ext}$  is the applied external voltage. If  $V_{BI}$  is unknown, then this introduces additional uncertainty. The relative uncertainty is reduced in thicker films where higher applied voltages are used. The value of  $\epsilon$  is also difficult to measure, though most organic semiconductors have dielectric constants in the range  $3.0\epsilon_0 < \epsilon < 4.0\epsilon_0$ , where  $\epsilon_0$  is the permittivity of free space. Typically a relative dielectric constant of  $3.5\epsilon_0$  is assumed, as is used in this work.
- *Charge trapping:* Traps are present in organic semiconductors as a result of disorder, contamination, defects, or degradation. They have been identified as a particular issue for electron transport in polymers [41,43]. When charge traps are present in a system, a portion of charge carriers will be trapped, while the remainder will be free to move. The ‘effective mobility’ is an average mobility that includes both free and trapped carriers. If the ratio of free carriers to trapped carriers is independent of voltage, then the SCLC method applies using the effective mobility. Many models, however, predict that the proportion of free carriers increases with voltage as deep traps become completely filled [30,31,16,40]. This creates a ‘trap-filling’ region of the  $I$ – $V$  curve in which the current rises exponentially or as a power-law function of voltage. Eq. (3) will not fit to this region. The field-dependence of mobility in this equation will, however, cope with the effects of shallow traps where the effective barrier to transport is reduced by the application of an electric field.
- *Doping:* Ionised dopants may be present in significant quantities in organic semiconductors. Although they

do not suffer the effects of coordination defects found in inorganic semiconductors, they are generally thought to be caused by contaminants, and are likely to be mobile. For example, reversible doping by oxygen can create an ionised acceptor population of greater than 0.1% of monomer units in polythiophenes [44]. When doping is of the right polarity (i.e. p-type in hole-only devices or n-type in electron-only devices), the main effect of doping is to increase Ohmic conductivity at low fields. Usually this Ohmic region of the  $I$ – $V$  curve is easily ignored. Doping of the wrong type (n-type in hole only devices), the dopants act as deep traps, leading to the trap-filling regime regime above that has a similar effect on  $I$ – $V$  curves as an increased built-in voltage. Some researchers have argued that the SCLC effect is masked by field-dependent ionisation of impurities (the Frenkel effect) [45,46], although this was ruled out on the devices measured in this article by testing the thickness dependence of the current.

#### 4. Variation in SCLC mobility benchmark measurements

In this section we discuss the reproducibility of measurements that are designed to extract a representative single benchmark value for mobility from a single measurement. This is aimed at applications where mobility is to be used as a comparator, for example for material screening. While it is possible to use more complex multi-parameter models to extract a more detailed picture of charge transport (e.g. trap and dopant concentrations, disorder, etc.), such models require more data, and have more subjective interpretation in terms of model selection and validation, that complicates comparison between materials.

To test the reproducibility of using SCLC to extract benchmark mobility values, we conducted a small inter-laboratory study summarised in Fig. 2. 21 pairs of hole-only sandwich-type devices were fabricated (different materials, different thicknesses, and with/without MoO<sub>3</sub> interlayer), with each pair consisting of two nominally identical devices (fabricated sequentially using the same polymer solution). The devices were sent to two labs to be measured, with one of each pair going to each lab. The labs were given no instructions on how to measure the devices, and followed their own internal procedures. One lab used a Keithley 236 Source Measure Unit, while the other used a Keithley 2440 Source Meter to measure current–voltage curves. Both labs used their own software to collect data. The resulting current–voltage datasets were distributed to different scientists who were asked to extract a mobility value for each device. Again, no instructions were given on how to do this. Voltage polarity for fitting was chosen to give hole injection from the MoO<sub>3</sub> HIL when present, or PEDOT:PSS otherwise. The resulting mobility values were collated and statistically analysed.

The results, shown in Fig. 3, reveal some interesting findings. First we consider the effect of using a MoO<sub>3</sub> HIL to assist hole injection relative to PEDOT:PSS. For PEDOT:PSS, the approximate energy scheme in Fig. 1 predicts an energetic barrier to hole injection that progressively decreases from F8BT through TFB to PFB. When PEDOT:PSS

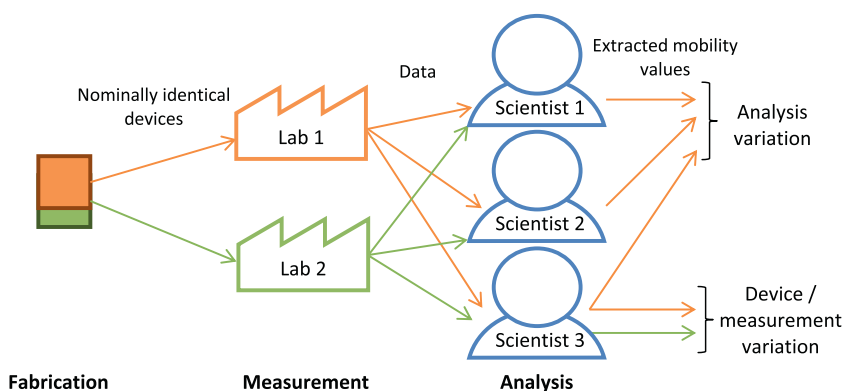


**Fig. 2.** Summary of interlaboratory comparison scheme used to measure nominally identical devices at different locations.

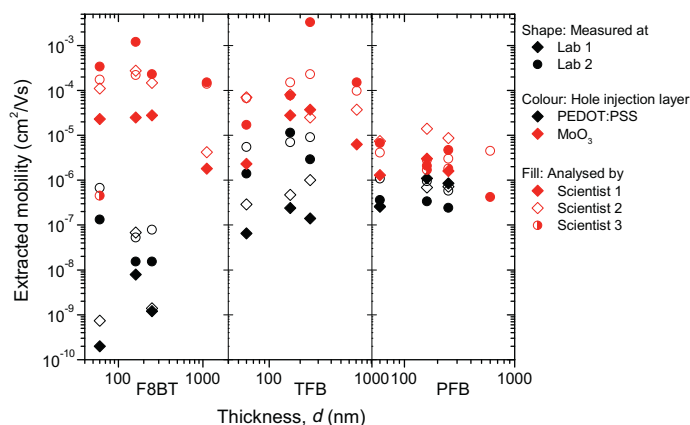


**Fig. 3.** Single device benchmark mobilities extracted using the SCLC Eq. (1) on current–voltage curves measured at two different laboratories and analysed by different scientists. Mobility is displayed as a function of device thickness for each of three different materials. The colour indicates whether charge injection was from  $\text{MoO}_3$  or PEDOT:PSS HIL. The shape indicates which laboratory the devices were measured in, and the shape fill indicates which scientist analysed the data. (For interpretation of the references to colour in this figure legend, the reader is referred to the web version of this article.)

was used as the hole-injecting contact, measured current densities were found to decrease progressively through this sequence. In contrast, the current densities measured when using the high work-function  $\text{MoO}_3$  HIL as a hole-injecting contact were much higher and did not follow this sequence. Moreover, the difference in current between the different electrodes was as much as 5 orders of magnitude with F8BT, whereas it was only about one order with PFB. When positive voltage was applied to the Au electrode in devices without  $\text{MoO}_3$  HILs, the measured current was very small, confirming that electron injection from PEDOT:PSS is not an issue when using a PEDOT:PSS/polymer/ $\text{MoO}_3$ /Au hole-only device structure with positive voltage applied to the  $\text{MoO}_3$  electrode. These findings strongly indicate that using PEDOT:PSS as the HIL results in injection limited behaviour. For these measurements, the mobility values extracted from the  $I$ – $V$  curves are not true; the assumption of efficient charge injection was not met, and hence the SCLC model is invalid. Often, in these cases, the fit of the SCLC model to the data will be poor and the measurement will be rejected. However, it is not always possible to determine injection-limited behaviour from a single  $I$ – $V$  curve; global fitting to test for the correct thickness depen-

dence is a useful tool for eliminating injection-limited devices.

A more surprising finding is the range of variation between the results. Variations of sometimes more than one order of magnitude were seen between matching devices measured in different locations and analysed by the same scientist, particularly where the devices were strongly injection-limited. Even more striking is the finding that, when the same data were analysed by different scientists, the human factor in analysing the data sometimes leads to variations of more than a factor of 10.

These data clearly highlight the need for harmonisation of experimental procedure, including device handling and measurement, but also for harmonisation in the interpretation of data. To encourage some progress in this area, we developed a protocol for analysing and reporting SCLC mobilities from single  $I$ – $V$  curves. The protocol, included in the [supplemental information](#) [14], compensates for some likely causes of uncertainty such as field-dependent mobility, series resistance, and built-in voltage. While many scientists currently employ similar protocols, they are not always formalised and reported.



The protocol proceeds in several stages. Firstly, the data to be fitted are selected. Secondly, the user checks for the presence of series resistance and either compensates for this or removes the affected data points. Thirdly, the user estimates the built-in voltage. Next, the region of the curve most likely to represent SCLC behaviour is selected, and is fitted using Eq. (3). Finally, the mobility is calculated at a specified electric field and recorded. This final step is important as it reduces the two-parameter model, in which there is a strong covariance between the two parameters to a single parameter that can be more reliably compared between different materials. The electric field to be used for comparison is selected to be relevant to the intended application.

We have tested the protocol by generating  $I$ - $V$  curves using a drift-diffusion device simulator including combinations of charge trapping, doping, energetic disorder and built-in voltage. When plotted on double-logarithmic axes, almost all  $I$ - $V$  curves comprise two or three distinct regions. At low voltages, the current increases linearly with voltage. This Ohmic region can be caused by the conduction of ‘intrinsic’ free charge carriers that are present in the semiconductor to compensate ionised dopants or have diffused from the electrodes. This region can be used to estimate the density of ‘intrinsic’ free carriers and can be a measure of the degree of doping present in the material. However, care is needed as other intrinsic and extrinsic effects, such as diffusion currents and pin-hole defects or other leakage paths also contribute to the Ohmic region. At higher voltages, we have the SCLC region following approximately  $J \propto V^\lambda$  where the value of  $\lambda$  is close to 2, or (often) increases with voltage due to field-activated mobility. The aim of the protocol is to use this region for fitting. In many cases, there is a third region of the  $I$ - $V$  curve at intermediate voltages for which  $\lambda \gg 2$ . This is explained by either built-in voltage or by the filling of deep trap states. Kirchartz and Beilstein [47] pointed out that deep charge traps act effectively as an additional barrier that has a similar effect on  $I$ - $V$  curves as built-in voltage. Our own simulations confirmed this, and we found that the protocol compensated for trapping to some extent by treating it as built-in voltage.

It is important to note that the benchmark mobility value that is extracted by the protocol is an ‘effective mobility’ that averages to some extent over trapped and free carriers. When traps were added to simulations, the corresponding benchmark mobility value extracted by the protocol was reduced. While, in many cases, researchers may wish to extract a theoretical free-carrier mobility for an ideal material, the ‘effective mobility’ is arguably more relevant to determining device performance. Thus, the benchmark mobility can be used as a comparator for the quality of a material.

The protocol was trialled by repeating the data analysis, this time asking the scientists to apply the protocol. One important aspect of the protocol is that it uses a field-dependent mobility, but asks the scientists to report the mobility at a pre-specified electric field, thus harmonising conditions between measurements where different voltage ranges were used. The results are shown in Fig. 4.

It is clear that the use of the protocol vastly reduces the variation due to both human factors and due to device and measurement variations. The latter is in part due to the compensation of built-in voltage, which apparently varies depending on measurement set up or environment. This is possibly due to variations in measurement protocol, such as voltage sweep rate, preconditioning, etc. The reduced measurement variation now allows clear trends in the plot of mobility against thickness to be seen. The apparent increase in mobility with increasing thickness when using PEDOT:PSS is a clear indication of injection-limited behaviour. The same is seen with MoO<sub>3</sub> HIL in thin devices, but the invariance of mobility at thicknesses above ~150 nm confirms the SCLC behaviour.

The effect of using the protocol on the variation of extracted mobility benchmark is analysed in Fig. 5. The variation was calculated by pooling the standard deviations of comparisons of nominally identical devices measured at different locations and analysed by the same scientist (device/measurement variation) and of comparisons of identical datasets analysed by different scientists (human analysis variation). Geometric standard deviation (GSD) is used to quantify the variations. GSD is a useful statistical concept to describe the distribution of random values spanning orders of magnitude (in which case regular

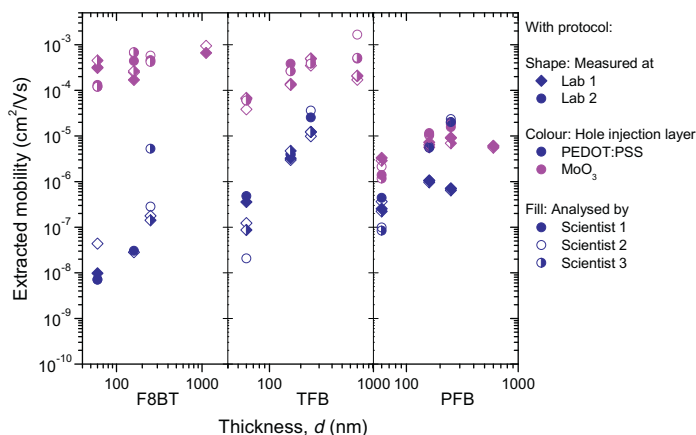
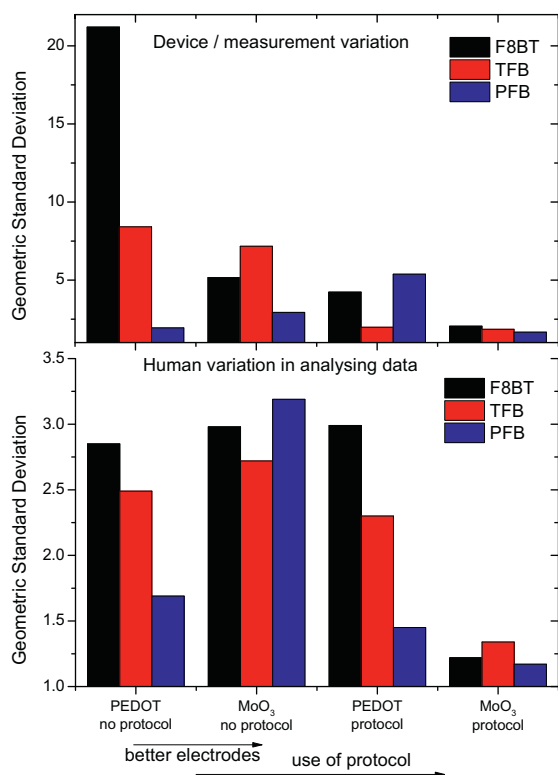


Fig. 4. Single device benchmark mobilities extracted from the same data as Fig. 3 using the proposed protocol [14] at an electric field of  $2.5 \times 10^5$  V/cm.



**Fig. 5.** The geometric standard deviation for two types of variation between benchmark mobilities measured with and without MoO<sub>3</sub> HIL and analysed with and without the protocol. The reproducibility of results is greatly improved by using good electrodes and an analysis protocol.

standard deviations become meaningless). The GSD is the multiple by which values typically vary. For example, assuming that measured mobilities have a lognormal distribution, then a GSD of 1.05 indicates that 68% of values are expected to be within  $\pm 5\%$  of the geometric mean; a GSD of 10 indicates that 68% of values are expected to lie between  $1/10$  and  $10\times$  the geometric mean.

Although there is some randomness in the results due to the relatively small sample size, there are some interesting points to note. The analysis shows that the typical device/measurement variation is very large (more than a factor of 20) when hole injection is poor and an analysis protocol is not used. When the protocol and a good HIL are used in conjunction, the device/measurement variation is reduced to a factor of about 2. The variation in mobility benchmark values extracted by different scientists (human variation) from the same data was typically a factor of 2.5–3.0 when a protocol was not used, but is reduced to about 1.2 (20% variation) with the use of the protocol.

The device/measurement variation is a problem in applications where materials, formulations or processes are to be compared to determine which is best. As each measurement has significant uncertainty, the confidence in the comparison is poor when the difference in measured mobility benchmarks is similar or less than the measurement variation. For example, if the GSD for device/measurement variation is 2.0 and only one device of each type is measured, the measured mobility in one device

must exceed that of the other by a factor of about 5 for the user to be 95% confident that its mobility is in reality higher [48,49]. (Generally 95% confidence is considered to be the threshold for statistical significance.) To improve the comparison, multiple (nominally identical) devices should be made and measured, and the geometric mean of the extracted mobility benchmarks taken. The reproducibility of this mean value improves as  $1/\sqrt{N}$  when  $N$  measurements are averaged. The repeated measurements should be used to evaluate the GSD for the measurement, provided at least 5–10 measurements are made ('Type A uncertainty evaluation') [49].

## 5. Uncertainty analysis

Besides using an analysis protocol, further reductions in measurement variation should be made by harmonising device fabrication and measurement procedures. Understanding from where the uncertainty arises can help. A simple Monte-Carlo uncertainty simulation of the device fabrication and measurement process was performed. Sets of device parameters were picked at random from the probability distributions listed in Table 1. For each set of

**Table 1**  
Probability distribution parameters used to generate device parameters for Monte-Carlo uncertainty analysis. All distributions were assumed to be Gaussian.

| Parameter                                   | Mean value                                   | Standard uncertainty   |
|---|--|------------------------|
| Material mobility, $\mu_0$                  | $10^{-6} \text{ cm}^2/\text{V s}$            | None                   |
| Field dependence, $\gamma$                  | $4.6 \times 10^{-3} \text{ cm}^2/\text{V s}$ | None                   |
| Mobility at $2.5 \times 10^5 \text{ V/cm}$  | $10^{-5} \text{ cm}^2/\text{V s}$            | None                   |
| Active layer film thickness                 | 250 nm                                       | $\pm 25 \text{ nm}$    |
| Active device area                          | 4 mm <sup>2</sup>                            | $\pm 0.8 \text{ mm}^2$ |
| Device series resistance                    | 50 $\Omega$                                  | $\pm 10 \Omega$        |
| Device shunt resistance                     | 10 M $\Omega$                                | None                   |
| Built-in voltage V <sub>BI</sub>            | 0 V  | $\pm 0.1 \text{ V}$    |
| Human error in estimating V <sub>BI</sub>   | 0 V  | $\pm 0.025 \text{ V}$  |
| Human error in estimating series resistance | 0 $\Omega$                                   | $\pm 5 \Omega$         |

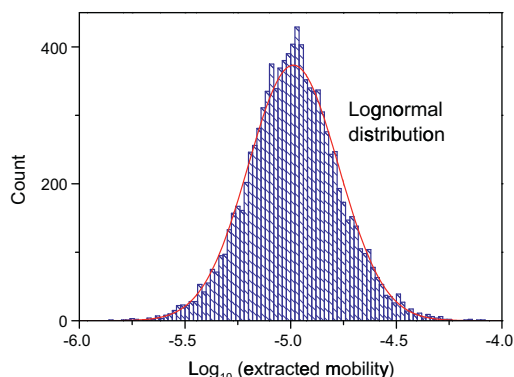


**Fig. 6.** Histogram of benchmark mobilities resulting from Monte-Carlo simulation of 10,000 devices. A lognormal distribution fit is shown for comparison (red line). (For interpretation of the references to colour in this figure legend, the reader is referred to the web version of this article.)

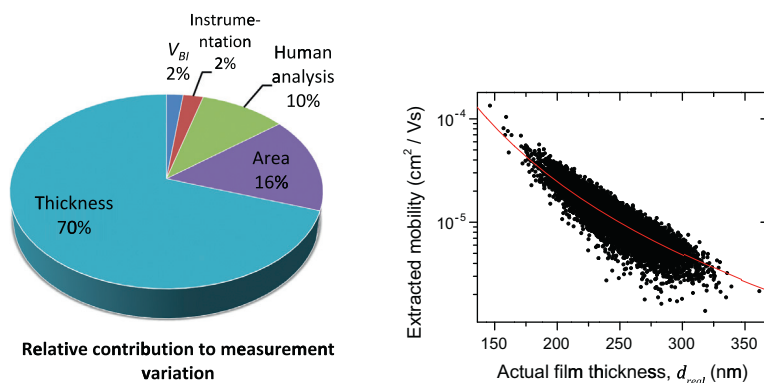


**Fig. 7.** Analysis of contributions to device/measurement variation in SCLC mobility benchmark measurements of approximately 250 nm-thick films. Left: pie chart of relative contribution of different causes of measurement variation. Right: Scatter plot of extracted mobility versus film thickness for 10,000 simulated devices. A thickness of 250 nm was assumed in each case when applying the mobility benchmarking protocol. Red line is the analytical expression  $\mu = \mu_0 \left( \frac{250 \text{ nm}}{d_{\text{real}}} \right)^3 \exp \left[ \gamma \left( 0.109 \sqrt{F} + 0.891 \right) \sqrt{F \frac{250 \text{ nm}}{d_{\text{real}}}} \right]$ . (For interpretation of the references to colour in this figure legend, the reader is referred to the web version of this article.)

parameters, a current–voltage curve was generated using Eq. (3) combined with a simple circuit model for series and shunt resistance (electrode/contact resistance and intrinsic conductance/leakage respectively) and with added noise and voltage/current errors randomly generated based on manufacturers specifications for a Keithley 2440 Source Meter. The generated current–voltage curves were then fed into a spread sheet used for applying the protocol for mobility extraction. Human error in the estimation of the built-in voltage and series resistance were also included as random variables. The benchmark mobility at a field of  $F = 2.5 \times 10^5 \text{ V/cm}$  was extracted for each of 10,000 randomly generated current–voltage curves, and the results are summarised in a histogram in Fig. 6.

The resulting values fall into a lognormal distribution with the geometric mean giving the correct mobility value and a GSD of 1.65, similar to that measured in the best cases above. The relative contribution of different sources of error to the variation in measured benchmark mobility is shown in Fig. 7. By far the largest contribution to the measurement variation arises from uncertainty in the device thickness. Note that it is assumed that the scientist analysing the data knows only the mean film thickness and device area of the whole set of devices, not the actual values for each device. Similarly, in our experiments above, the thickness of each individual film was not measured. Instead the typical thickness of a film prepared under the same conditions is used in analysing the data. A scatter plot is included in Fig. 7 that illustrates the strong correlation between extracted mobility and actual film thickness (note that the strong non-linearity precludes analysis using a standard linearized uncertainty model). This study suggests that a significant improvement in the reliability of mobility benchmark studies can be achieved by accurately measuring the film thickness of the actual devices to be measured, or by improving the consistency of film preparation.

## 6. Conclusions and recommendations

In general, full description of charge transport requires models going beyond the simple concept of mobility that

reconcile the differences between techniques and simulate the measurement process itself [28,50]. However, such models are complex and require significantly more data and expertise than are often available to small enterprises and research groups. For screening applications, where the aim is to compare charge mobility in different materials, processes or formulations, it is useful to obtain a single benchmark parameter for charge-carrier mobility from a simple experiment. Therefore measurement reproducibility is key. Our work illustrates that different techniques and measurement conditions yield wildly varying results. Consistency in experimental method is therefore crucial. In addition, it is desirable to acquire only a minimal set of data and to apply only simple analysis. For example, it is common to extract a mobility measurement from a single  $I$ – $V$  curve taken on a single device, without comparing, for example, different film thicknesses. We refer to such a measurement as a ‘benchmark’ measurement. It is to be understood that a mobility benchmark value is only indicative. It can be used for comparisons between similar materials, but should not be considered rigorous, and should not be compared with mobilities extracted using different techniques or under different experimental conditions.

From the large number of experimental techniques in use to measure charge mobility in organic semiconductors, we have found that steady-state SCLC measurements are simple and versatile. The equipment requirements are modest, and the device design is conventional, and films of similar thickness to OPV and OLED device can be used. The availability of current meters with large dynamic ranges allows the measurement of a wide range of semiconductor materials. Furthermore, as the measurement is steady state, it is representative of equilibrium transport and implicitly measures charge trapping. The greatest experimental challenge with SCLC is in ensuring that the transport is bulk limited rather than injection limited. This can particularly be an issue when measuring electron transport. The choice of injection layer is crucially important to making SCLC measurements in unipolar devices. When the injection-limited behaviour cannot be categorically ruled out, the extracted



mobility value should be considered to be a lower limit of the true mobility.

For material comparisons, we recommend that organisations follow a protocol for device preparation and measurement, taking particular care of the reproducibility and measurement of device thickness. It is hard to specify a general protocol for all situations, however, we recommend paying attention to the following points for making SCLC mobility benchmark measurements:

1. Ensure that the current is not injection limited by using good electrodes or injection layers, and that the thickness is appropriate.
2. Always use a protocol for data analysis and reporting such as the one proposed here [14].
3. Ensure that device fabrication is consistent, paying particular attention to film thickness; measure film thickness of the actual measured devices when practicable.
4. Ensure that the bias voltage polarity is correct for best injection.
5. Use mechanically stable electrical connections.
6. For current–voltage curves, begin sweeping from zero volts to avoid bias stress and transient effects. Use a return sweep to test for hysteresis and vary sweep rate/source-measure delay to minimise hysteresis. Repeat measurements several times, until the results are repeatable, before extracting mobility values (e.g. sweep sequence  $0V \rightarrow +V_{max} \rightarrow 0V \rightarrow -V_{max} \rightarrow 0V$ , hold, repeat).
7. Adjust voltage sweep range with thickness as necessary to measure at desired electric field range.
8. Measure under consistent environmental conditions (controlled temperature, dark conditions, constant humidity / encapsulation).
9. When introducing new materials, different device structures, etc., it is important to verify that the SCLC conditions are met by verifying that the thickness-dependence of current density is correct. This can be done either by global fitting of  $I$ – $V$  curves on devices of different thickness, or by comparing the mobilities extracted using the protocol on devices of different thickness. As seen with injection from PEDOT:PSS above, an apparent dramatic increase in mobility with increasing film thickness indicates injection-limited behaviour and these data should be rejected.

Most importantly, users should quantify the reproducibility of their results by repeating the entire device fabrication, measurement and analysis process several times, and use this to determine the appropriate sample size to use for material comparisons. The importance of statistics should never be overlooked. A good discussion of this point was made recently in the context of OPV efficiency [51], and literature on appropriate methods is freely available [49]. Nevertheless, one must bear in mind that repetition affects precision rather than accuracy, and benchmark measurements performed using different procedures might never be comparable. Therefore it is crucial that an internationally standardised procedure for mobility benchmark measurements be developed.

The investigation presented in this work is a first step in this direction. We identified the main sources of uncer-

tainty in device reproducibility (i.e. active layer thickness and active area) and we demonstrated that, surprisingly, a very large component of lack of reproducibility of results arose from different ways of interpreting data. We developed a simple protocol for analysis and reporting that was found to greatly improve the reproducibility of results. The protocol introduced here is shared with the community as a starting point to improve harmonisation, and we encourage the community to experiment and improve upon it. New versions and discussions of the protocol are hosted on the NPL website [52].

## Acknowledgements

This work was funded through the European Metrology Research Programme (EMRP) Project IND07 Thin Films. The EMRP is jointly funded by the EMRP participating countries within EURAMET and the European Union.

C. Arantes, R. Valaski and M. Cremona are grateful to the Brazilian agencies CNPq, FAPERJ, INCT-INEO for financial support.

## Appendix A. Supplementary material

Supplementary data associated with this article can be found, in the online version, at <http://dx.doi.org/10.1016/j.orgel.2014.02.008>.

## References

- [1] V.D. Mihailetschi, H.X. Xie, B. de Boer, L.J.A. Koster, P.W.M. Blom, *Adv. Funct. Mater.* 16 (2006) 699.
- [2] S.R. Cowan, R.A. Street, S. Cho, A.J. Heeger, *Phys. Rev. B* 83 (2011) 035205.
- [3] W. Tress, K. Leo, M. Riede, *Phys. Rev. B* 85 (2012) 155201.
- [4] M. Lenes, M. Morana, C.J. Brabec, P.W.M. Blom, *Adv. Funct. Mater.* 19 (2009) 1106.
- [5] L.S. Hung, C.H. Chen, *Mater. Sci. Eng., R* 39 (2002) 143.
- [6] J.C. Blakesley, H.S. Clubb, N.C. Greenham, *Phys. Rev. B* 81 (2010) 045210.
- [7] N. Vukmirović, L.-W. Wang, *J. Phys. Chem. B* 113 (2009) 409.
- [8] V. Rühle, J. Kirkpatrick, D. Andrienko, *J. Chem. Phys.* 132 (2010) 134103.
- [9] S.L.M. van Mensfoort, R. Coehoorn, *Phys. Rev. B* 78 (2008) 085207.
- [10] A. Kokil, K. Yang, J. Kumar, *J. Polym. Sci., Part B: Polym. Phys.* 50 (2012) 1130.
- [11] H. Scher, E.W. Montroll, *Phys. Rev. B* 12 (1975) 2455.
- [12] C. Tanase et al., *Phys. Rev. Lett.* 91 (2004) 216601.
- [13] H. Sirringhaus, M. Bird, T. Richards, N. Zhao, *Adv. Mater.* 22 (2010) 3893.
- [14] <http://www.npl.co.uk/science-technology/electrochemistry/research/organic-electronics/mobility-protocol>.
- [15] S.L.M. van Mensfoort, S.I.E. Vulto, R.A.J. Janssen, R. Coehoorn, *Phys. Rev. B* 78 (2008) 085208.
- [16] H.T. Nicolai, G.A.H. Wetzelaer, M. Kuik, A.J. Kronemeijer, B. de Boer, P.W.M. Blom, *Appl. Phys. Lett.* 96 (2010) 172107.
- [17] A.M. Nardes, M. Kemerink, M.M. de Kok, E. Vinken, K. Maturova, R.A.J. Janssen, *Org. Electron.* 9 (2008) 727 <<http://www.heraeus-clevios.com/>>.
- [18] W. Osikowicz, M.P. de Jong, S. Braun, C. Tengstedt, M. Fahlman, W.R. Salaneck, *Appl. Phys. Lett.* 88 (2006) 193504.
- [19] I. Lange, J.C. Blakesley, J. Frisch, A. Vollmer, N. Koch, D. Neher, *Phys. Rev. Lett.* 106 (2011) 216402.
- [20] I. Irfan, A.J. Turinske, Z. Bao, Y. Gao, *Appl. Phys. Lett.* 101 (2012) 093305.
- [21] D. Kabra, L.P. Lu, M.H. Song, H.J. Snaith, R.H. Friend, *Adv. Mater.* 22 (2010) 3194.
- [22] H. Bässler, *Phys. Status Solidi B* 175 (1993) 15.
- [23] D. Hertel, H. Bässler, *Chem. Phys. Chem.* 9 (2008) 666.

- [24] A.B. Walker, A. Kambili, S.J. Martin, J. Phys.: Condens. Matter 14 (2002) 9825.
- [25] J.M. Marshall, Rep. Prog. Phys. 46 (1983) 1235.
- [26] J. Orenstein, M. Kastner, Phys. Rev. Lett. 46 (1981) 1421.
- [27] D. Monroe, Phys. Rev. Lett. 54 (1985) 146.
- [28] M. Schubert, E. Preis, J.C. Blakesley, P. Pingel, U. Sherf, D. Neher, Phys. Rev. B 87 (2013) 024203.
- [29] R.P. Rocha, J.A. Freire, J. Appl. Phys. 112 (2012) 083717.
- [30] H.T. Nicolai, M.M. Mandoc, P.W.M. Blom, Phys. Rev. B 83 (2011) 195204.
- [31] J. Dacuna, W. Xie, A. Salleo, Phys. Rev. B 86 (2012) 115202.
- [32] G. Juska, K. Arlauskas, M. Viliunas, J. Kocka, Phys. Rev. Lett. 84 (2000) 4946.
- [33] A. Many, G. Rakavy, Phys. Rev. 126 (1962) 1980.
- [34] T.S. Esward et al., J. Appl. Phys. 109 (2011) 093707.
- [35] R. Steyrleuthner, M. Schubert, F. Jaiser, J.C. Blakesley, Z. Chen, A. Facchetti, D. Neher, Adv. Mater. 22 (2010) 2799.
- [36] J.C. Blakesley, M. Schubert, R. Steyrleuthner, Z. Chen, A. Facchetti, D. Neher, Appl. Phys. Lett. 99 (2011) 183310.
- [37] G.A.H. Wetzelaer, A. Najafi, R.J.P. Kist, M. Kuik, P.W.M. Blom, Appl. Phys. Lett. 102 (2013) 053301.
- [38] N.F. Mott, R.W. Gurney, Electronic Processes in Ionic Crystals, Oxford University Press, Oxford, 1940.
- [39] P.N. Murgatroyd, J. Appl. Phys. D 3 (1970) 151.
- [40] P. Mark, W. Helfrich, J. Appl. Phys. 33 (1962) 205.
- [41] R. Steyrleuthner, S. Bange, D. Neher, J. Appl. Phys. 105 (2009) 064509.
- [42] Z.B. Wang, M.G. Helander, M.T. Greiner, J. Qiu, Z.H. Lu, Phys. Rev. B 80 (2009) 235325.
- [43] H.T. Nicolai, M. Kuik, G.A.H. Wetzelaer, B. de Boer, C. Campbell, C. Risko, J.L. Brédas, P.W.M. Blom, Nat. Mater. 11 (2012) 882.
- [44] G. Lu et al., Nat. Commun. 4 (2013) 1588.
- [45] X.-G. Zhang, S.T. Pantelides, Phys. Rev. Lett. 108 (2012) 266602.
- [46] B.A. Gregg, S.E. Gledhill, B. Scott, J. Appl. Phys. 99 (2006) 116104.
- [47] T. Kirchartz, J. Beilstein, Nanotechnology 4 (2013) 180.
- [48] The GSD of the ratio of mobilities is  $GSD_{12}+GSD_{22}$  where GSD1 is the GSD of the first mobility etc., and we have used the rule that 95% of a lognormal probability distribution lies in the interval  $[\text{geometric mean}/(1.65 \times GSD), \text{infinity}]$ .
- [49] For further information on measurement uncertainty, we refer readers to the Guide to Uncertainty in Measurement, which is available free of charge from the BIPM, <<http://www.bipm.org/>>.
- [50] M.T. Neukom, S. Züflea, B. Ruhstaller, Org. Electron. 13 (2012) 2910.
- [51] E.J. Luber, J.M. Buriak, J. Am. Chem. Soc. Nano 7 (2013) 4708.
- [52] <http://www.npl.co.uk/science-technology/electrochemistry/research/organic-electronics/mobility-protocol>.